Journal of Molecular Structure 1197 (2019) 73–79

Contents lists available at ScienceDirect

Journal of Molecular Structure

journal homepage: http://www.elsevier.com/locate/molstruc

A new coumarin-based fluorescence “turn-on” sensor for Al(III) ions and its bioimaging in cell

Lei Jin [a], Wenling Wang [a, *], Zheyu Shen [a], Jiahao Xu [a], Qingming Wang [a, **], Chengying Zhao [b, ***]

[a] *School of Pharmacy, Yancheng Teachers' University, Yancheng, Jiangsu, 224051, China*
[b] *Institute of Food Science and Technology, Chinese Academy of Agricultural Sciences, Beijing, 100193, China*

ARTICLE INFO

Article history:
Received 18 December 2018
Received in revised form
9 July 2019
Accepted 10 July 2019
Available online 11 July 2019

Keywords:
Aluminum ion
Fluorescence probe
Fluorescence turn - on
Coumarin-based
Bioimaging

ABSTRACT

A new coumarin-based probe 3-acetyl-7-diethylaminocoumarinthiosemicarbazone (**DCT**) is synthesized for Al^{3+} fluorescence detection in CH_3CH_2OH/H_2O (6 : 4, *v*/*v*). The fluorescence intensity at 428 nm was enhanced about 15-fold with the fluorescence changed from colorless to blue. The binding constantof Al^{3+} with **DCT** is $5.04 \times 10^6\ M^{-1}$. The limit of detection (LOD) of Al^{3+} is calculated to be 82 nM. Furthermore, the binding details are determined by Job’s plot and ESI - MS studies, which indicated that a stoichiometric ratio of 1 : 1 complex is formed between Al^{3+} and **DCT**. Cell imaging confirmed that **DCT** could useful for detecting Al^{3+} in HepG2 cells.

1. Introduction

As the third abundant element in the earth, Al^{3+} is universal used in food, alloy, packing material, and so onhttps://www.sciencedirect.com/science/article/pii/S1010603016302465, [1]. About 3–10 mg of Al^{3+} in daily intake is allowed on the basis of the World Health Organization https://www.sciencedirect.com/science/article/pii/S1010603016302465, [2]. Mnay adverse physiological effects and diseases (such as bone softening, microcytic hypochromic anemia, myopathy, encephalopathy and Alzheimer’s disease) could be caused by excess levels of Al^{3+} [3]. In addition, the aquatic life [4] and soils for agricultural production [5] could be hazarded by Al^{3+}. Therefore, detection of Al^{3+} is of great significance to prove the content of Al^{3+} in the environment and reduce the direct impact of Al^{3+} on human health [6].

Compared to the conventional techniques [7–9], fluorescent probes have received widely attention for detecting various anionic/cationic and others due to its fast response, high sensitivity and selectivity, low limit of detection, facile visualization and simple operation, real-time analysis, and non-destruction [10–18]. Various fluorescent probes via different strategies toward Al^{3+} detection have been reported [19–32], including calixarene [22,23], triazoles [24], rhodamine [31] and so on. Unfortunately, monitoring and detection of Al^{3+} faced multiple disadvantages (for example, sensing mechanisms only work at organic solvents or non-physiological pH), strong hydration, poor coordination ability and a small Stokes shift [33–36]. Therefore, to design fluorescence probe for Al^{3+} is urgently demanded. For the favourable biocompatibility and photophysical properties, coumarin has been abroadly used as fluorophores in many fields and a lot of derivates were designed and synthesized [37,38].

Herein, we reported a new coumarin-based off-on fluorescent probe (**DCT**), which could be used for sensitive and selective of the detection of Al^{3+} in CH_3CH_2OH - H_2O (6 : 4, v/v). The structure of **DCT** was determined by IR spectra (IR) analysis, ^1H NMR and ^{13}C NMR, Electrospray ionization mass spectra (ESI - MS) (listed in Figs. S1–S4). A remarkably fluorescence intensity was enhanced and prominent color changes upon recognition was seen.

---

[*] Corresponding author.
[**] Corresponding author.
[***] Corresponding author.

E-mail addresses: wangwenl2018@163.com (W. Wang), wangqm@yctu.edu.cn (Q. Wang), zcyzhao@sina.com (C. Zhao).

https://doi.org/10.1016/j.molstruc.2019.07.048

2. Experimental section

2.1. Materials preparation

All the solvents and chemicals were of analytic grade. The cations (such as KCl, NaCl, $CaCl_2$, $MgCl_2 \cdot 6H_2O$, and so on) and the anions (such as KBr, NaCl, KI, Na_2SO_4, Na_3PO_4, NaH_2PO_4, NaOH, $NaHCO_3$, $NaNO_3$, NaBr, $Na_2C_2O_4 \cdot H_2O$) were obtained from Shanghai Experiment Reagent Co, Ltd (Shanghai, China). Other reagents were gained from Shanghai. The probe **DCT** was prepared in DMSO to obtain the stock solutions (1.0 mmol/L). The salts stock solutions were newly prepared by distilled water. NaClO was prepared from dilution of 10% solution in water.

2.2. Techniques and instruments

Bruker DRX 400 spectrometer with TMS as the internal standard was used to obtain the ^1H NMR and ^{13}C NMR spectra. NICOLET380 FT-IR spectrometer in KBr disks with the scanning speed 0.6329 cm/s was applied to recorded the FT-IR spectra (4000 - 400 cm^{-1}). VARI-EL elemental analyzer was used for recording Elemental analyses (EAs). A Triple TOF TM 5600$^+$ system with the positive ion model was used to obtain Electrospray ionization mass spectra (ESI - MS). All of the fluorescence spectral were recorded on a RF-5301 fluorescence spectrophotometer. UV-1800 ENG was applied to proceed the Ultraviolet spectrum. A confocal laser scanning microscope with model LSM-880 was used to fluorescence images on HepG2 cells.

2.3. Synthesis of DCT

*2.3.1. Synthesis of 3-acetyl-7-diethylaminocoumarin(**DC**)*

3-Acetyl-7-diethylaminocoumarin (**DC**) and 3-acetyl-7-diethylaminocoumarinthiosemicarbazone (**DCT**) were synthesized according the reported methods [39–41], as shown in Scheme 1. Briefly, 0.966 g (5 mmol) of 4-(Diethylamino)salicylaldehyde and 0.646 g (5 mmol) of ethyl acetoacetate were added to 30 mL CH_3CH_2OH. Then drop-wise of morpholine and acetic acid into the above solution. After refluxed for 20 h with stirring constantly, the color was changed to dark green, then stop the reaction and cooled to room temperature, the yellow products was got. The products was collected and washed by CH_3CH_2OH and dried in vacuo with yield of 39.4% for **DC**. FT-IR (KBr, cm^{-1}): 3018(Ar - H), 2982 (C - H), 1752 (C = O), 1644, 1608 (Ar, C=C), 1236, 1182 (C-O-C). Exact mass for **DC**: 259.1208, ESI - MS (positive mode) [**DC** + Na^+]$^+$ (m/z,282.5092). Elemental analysis (calcd. %) for $C_{15}H_{17}NO_3$: C, 69.48; H, 6.61; N. 5.41; Found: C, 69.56; H, 5.94; N. 5.39.

*2.3.2. Synthesis of 3-acetyl-7-diethylaminocoumarinthiosemicarbazone(**DCT**)*

DCT was prepared by mixing of **DC** with thiosemicarbazide in 30 mL absolute CH_3CH_2OH. Then drop-wise a few of CH_3COOH into the above solution and the resulting solution was reflux for 12 h. After ended the reaction, the dark brown color product was obtained and recrystallized by CH_3CH_2OH. Dried in vacuum desiccator. FT-IR (KBr, cm^{-1}): 3461 (N-H), 2982 (C - H), 1732 (C = O), 1611, 1556, (Ar, C=C), 1210, 1145 (C-O-C). Exact mass for **DCT**: 332.1307, ESI - MS (positive mode) [**DCT** + H^+]$^+$ (m/z, 333.6915), [**DCT** + Na^+]$^+$ (m/z, 356.0378). Elemental analysis (calcd. %) for $C_{16}H_{20}N_4O_2S \cdot 0.2CH_3CH_2OH$: C, 57.66; H, 6.25; N, 16.40; Found: C, 57.62; H, 6.02, N, 6.25. ^1H NMR (400 MHz, DMSO) δ 11.07 (s, 1H), 9.49 (s, 1H), 8.19 (s, 1H), 7.87 (s, 1H), 7.66 (s, 1H), 7.51 (d, J = 8.8 Hz, 1H), 6.20 (dd, J = 8.9, 2.3 Hz, 1H), 6.09 (d, J = 2.4 Hz, 1H), 3.32 (q, J = 7.1 Hz, 6H), 1.09 (t, J = 7.0 Hz, 7H). ^{13}C NMR (101 MHz, DMSO) δ 177.18, 176.39, 158.70, 150.76, 142.83, 129.79, 107.71, 104.25, 97.95, 44.29, 12.94.

3. Results and discussion

3.1. UV-vis absorption and fluorescence spectra of DCT towards Al^{3+}

The recognization behavior of probe **DCT** were studied in a CH_3CH_2OH - H_2O (6 : 4, v/v) system by spectroscopics. A solution of **DCT** (8.0 μM) was placed in a quartz cell (10.0 mm width) and 2 μL Al^{3+} (3×10^{-3} M) was drop-wised gradually, then the UV-vis spectra titration for Al^{3+} was obtained. As shown in Fig. 1, the absorption intensity at 402 nm was gradually decreased while the absorption intensity at 368 nm was increased with the increase of Al^{3+}. An isoabsorptive point at 382 nm was found. These results revealed that a new product was generated between **DCT** and Al^{3+} [42].

The changes of fluorescence emission spectra of **DCT** (1.0 μM) with the absence or presence of Al^{3+} (0–16 μM) in CH_3CH_2OH - H_2O (6 : 4, v/v) were listed in Fig. 2. A drastic fluorescence enhancement was exhibited with the increase of Al^{3+}. A new fluorescence peak at 428 nm was appeared. A fluorescence enhancement factor (FEF) is up to 15 - fold in the presence of 16 equiv. Al^{3+}. Interestingly, the Al^{3+} induced the fluorescence turn on for **DCT** with a color changed from colorless to blue under illumination with a 365 nm lamp (showed in Fig. 2 inset).

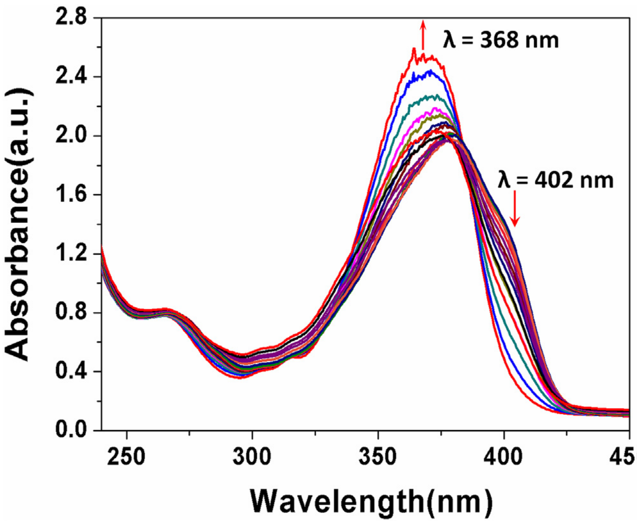

Fig. 1. Absorption titration of probe **DCT** (10 μM) with Al^{3+}(0–40 μM) in CH_3CH_2OH - H_2O (6 : 4, v/v) at room temperature.

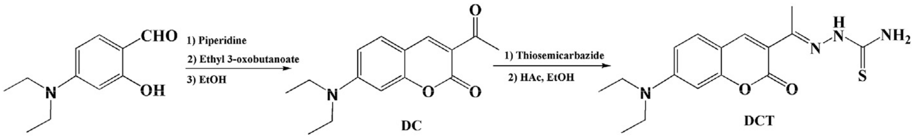

Scheme 1. Synthesis of probe **DCT**.

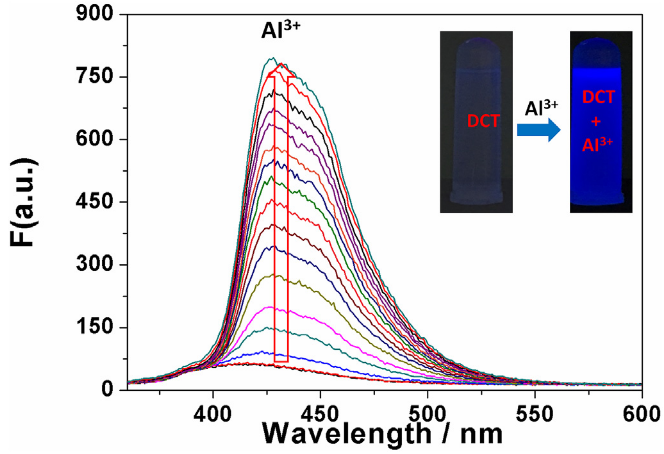

Fig. 2. Fluorescence spectra of **DCT** (1.0 μM) on addition of different amount of Al^{3+} (0–7.5 μM) in CH_3CH_2OH - H_2O (6 : 4, v/v). Inset: The visible fluorescence changes upon UV irradiation. ($\lambda_{ex} = 345$ nm).

By fluorescence titration, the sensitivity of **DCT** to Al^{3+} was decipted. As shown in Fig. S5, 1.0 μM of **DCT** were added with many different concentrations of Al^{3+} (0–8.0 μM) in CH_3CH_2OH - H_2O (6 : 4, v/v). The correlation coefficient of R^2 was 0.994. The detection limit (LOD) for Al^{3+} - **DCT** complex was calculated to be 82 nM. The results showed that **DCT** could be potentially applied to quantitative detection of Al^{3+}.

3.2. Selectivity studies

For practical applicability and to check the specificity on monitoring Al^{3+}, the possible interferences of other metal ions and anions were conducted by competitive experiments. The recognition ability of **DCT** for metal ions and anions in CH_3CH_2OH - H_2O (6 : 4, v/v) were studied. As shown in Fig. 3 and Fig. S6, the fluorescence spectrum of **DCT** was recorded when a lot of metal ions were added (10 equiv) in CH_3CH_2OH - H_2O (6 : 4, v/v). It could be easily to find that it is about enhanced 15- fold at 428 nm ($\lambda_{ex} = 345$ nm) with the presence of Al^{3+}. The other tested metal ions (such as Na^+, Mg^{2+}, K^+,Ba^{2+}, Ca^{2+}, Cr^{3+}, Fe^{3+}, Co^{2+},Ni^{2+}, Mn^{2+}, and so on), showed no obvious fluorescence enhancement when they were added to the solution of **DCT**. Thus, **DCT** exhibits well selectivity to Al^{3+} over other tested metal ions. As the same, competition experiments were carried out to detect Al^{3+} by **DCT** with the presence of anions (10 equiv.), such as NO_2^-, $H_2PO_4^-$, HPO_4^{2-}, $P_2O_7^{2-}$, PO_4^{3-}, SO_4^{2-}, $C_2O_4^{2-}$, $B_4O_7^{2-}$, and so on. As a result, the tested anions induced no remarkable influence on **DCT** to recognize Al^{3+}. (Fig. 4 and Fig. S7). All the results told us that **DCT** exhibited good selectivity for Al^{3+}.

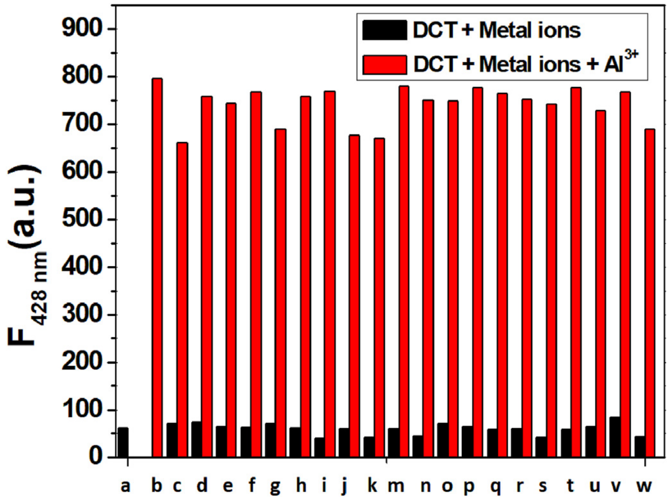

Fig. 3. Fluorescence intensity of **DCT** (1.0 μM) and its complexation with Al^{3+} in the presence of 20 aquiv. various metal ions in CH_3CH_2OH - H_2O (6 : 4, v/v). $\lambda_{ex} = 345$ nm, $\lambda_{em} = 428$ nm, slit: 3 nm/3 nm (Digital **a)-w)** respectively represents different metal ions: **a)**, **DCT**; **b)**, Al^{3+}; **c)**, Na^+; **d)**, K^+; **e)**, Mg^{2+}; **f)**, Ca^{2+}; **g)**, Ba^{2+}; **h)**, Cr^{3+}; **i)**, Co^{2+}; **j)**, Mn^{2+}; **k)**, Fe^{3+}; **m)**, Ni^{2+}; **n)**, Cu^{2+}; **o)**, Cd^{2+}; **p)**, Zn^{2+}; **q)**, Pb^{2+}; **r)**, Bi^{3+}; **s)**, Ag^+; **t)**, Sn^{2+}; **u)**, Sr^+; **v)**, NH_4^+; **w)**, Hg^{2+}.

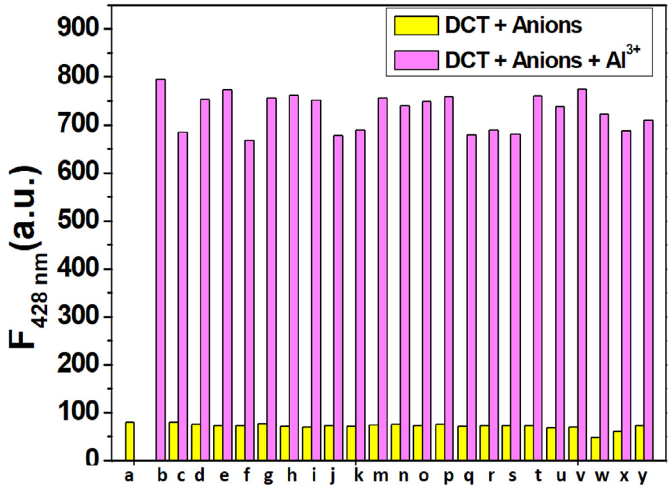

Fig. 4. Fluorescence intensity of **DCT** (1.0 μM) and its complexation with Al^{3+} in the presence of 20 aquiv. various anions in CH_3CH_2OH - H_2O (6 : 4, v/v). $\lambda_{e\ x} = 345$ nm, $\lambda_{em} = 428$ nm, slit: 3 nm/3 nm (Digital **a)-y)** respectively represents different anions: **a)**, **DCT**; **b)**, Al^{3+}; **c)**, NO_2^-; **d)**, $H_2PO_4^-$; **e)**, HPO_4^{2-}; **f)**, $P_2O_7^{2-}$; **g)**, PO_4^{3-}; **h)**, SO_4^{2-}; **i)**, $C_2O_4^{2-}$, **j)**, $B_4O_7^{2-}$; **k)**, CO_3^{2-}; **m)**, ClO_4^-; **n)**,NO_3^-; **o)**, SCN^-; **p)**, Ac^-; **q)**, F^-; **r)**, Ac^-; **s)**, Cl^-; **t)**, Br^-; **u)**, I^-; **w)**,CN^-; **x)**, HCO_3^-; **y)**, HSO_4^-

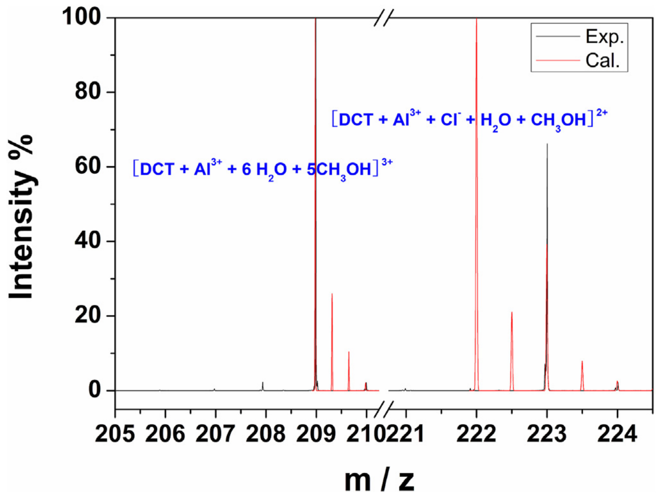

Fig. 5. ESI mass spectra of **DCT** upon addition of excess Al^{3+}.

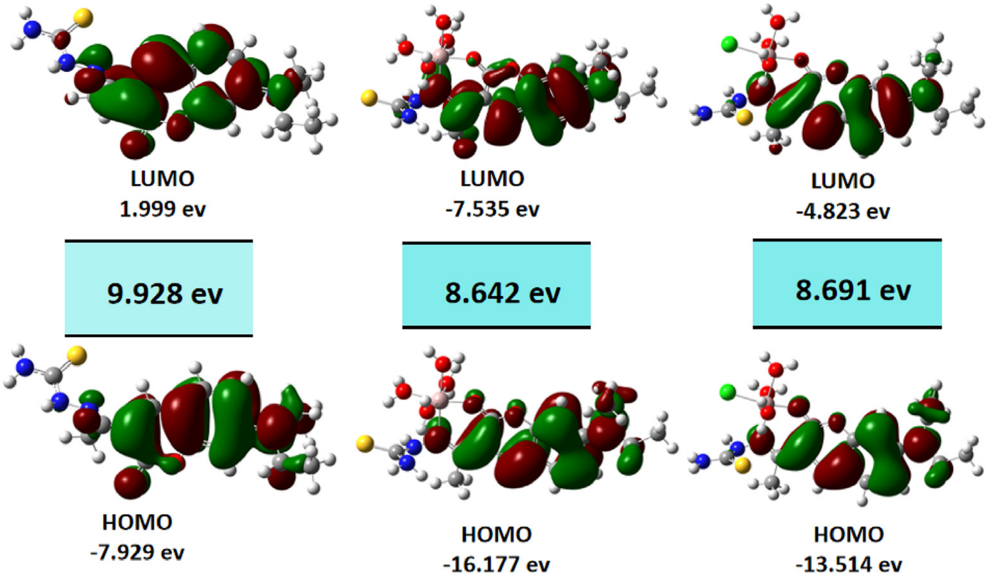

Fig. 6. HOMO and LUMO orbitals of **DCT** and Al^{3+}.

3.3. *Mechanism studies*

Mass spectral was widely used to verified the mechanism [43]. The binding stoichiometry of **DCT** and Al^{3+} was confirmed by mass spectral. The positive ion mass spectrum of **DCT** with addition of excess Al^{3+} (Fig. 5) showed two molecular ion peaks, a peak at 208.9964 can be assigned to [**DCT** $+ Al^{3+} + 6H_2O + 5CH_3OH]^{3+}$ (cal. For 209.0021), a peak *m*/*z* at 222.9996 can be calculated for [**DCT** $+ Al^{3+} + Cl^- + H_2O + CH_3OH]^{2+}$ (cal. For 222.9937). The results indicated the 1:1 complexes between Al^{3+} and **DCT** was formed. Job's plot was proceed by changing the ratio of Al^{3+} to obtain the accurate coordination stoichiometry between **DCT** and Al^{3+}. As shown in Fig. S8, the maximum fluorescence value is 0.48, followed by the plot of fluorescence intensity (F) versus $[Al^{3+}]/[Al^{3+}$+**DCT**], indicating a type of 1:1 complex was formed between Al^{3+} and **DCT**. Accordingly, the association constant for **DCT**-Al^{3+} complex ($K_b = 5.04 \times 10^6\ M^{-1}$) was calculated by Benesi-Hildebrand equation (Fig. S9).

The DFT calculations were used to analyze the sensing mechanism of Al^{3+} with **DCT**. The optimized structures of probe **DCT** and **DCT**-Al^{3+} complex are shown in Fig. 6 and Fig. 7. The Al^{3+} ion was six-coordinated with oxygen atom of one probe **DCT** and H_2O donor

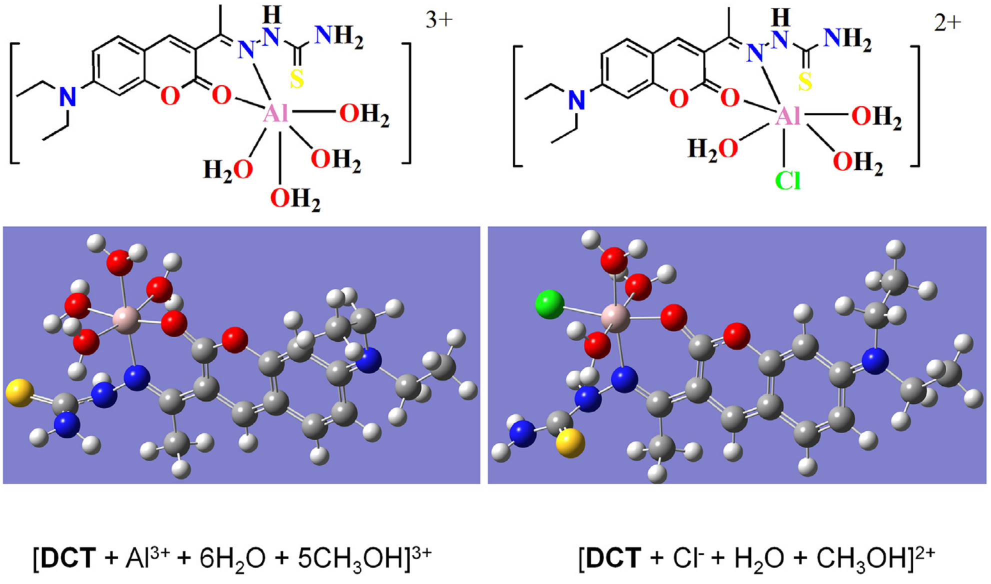

Fig. 7. The bond length of complexes between **DCT** and Al^{3+}.

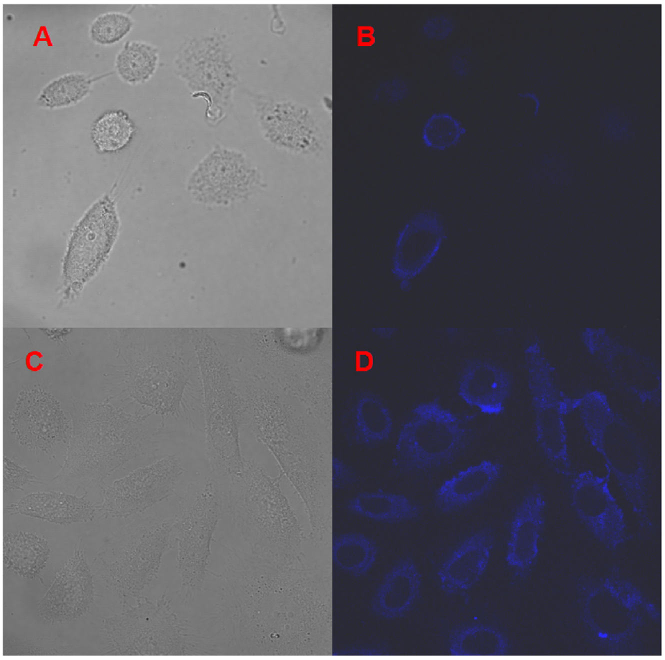

Fig. 8. Confocal fluorescence images in HepG2 cells.

set, and the bond lengths of Al-O were in the range of 1.80–2.03 Å, corresponding with mass peaks at 208.9964 ([**DCT** + Al^{3+} + $6H_2O$ + $5CH_3OH]^{3+}$). The coordination bond lengths of **DCT**-Al^{3+} complex with mass peaks at 222.99964 ([**DCT** + Al^{3+} + Cl^- + H_2O + $CH_3OH]^{2+}$) were in the range of 1.84–2.18 Å, which are in the range of typical coordination bond distances [42–45], indicating **DCT**-Al^{3+} complex is stable. The highest occupied molecular orbital (HOMO) and the lowest unoccupied molecular orbital (LUMO) of probe **DCT** and **DCT**-Al^{3+} complex were also conducted (Fig. 6). The results well confirmed the extent of intramolecular charge transfer (ICT) in **DCT** which were sufficient to reduce its fluorescence. Binding with Al^{3+} ions inhibited the electron transport of coumarin lactone ring, resulting in the fluorescence intensity enhanced by chelation-enhanced fluorescence (CHEF) mechanism [46–50].

3.4. *In-vitro cellular imaging*

To further explore the practical application in living cells, fluorescence imaging of **DCT** in HepG2 cells was proceed. The HepG2 cells were cultured following the reported methods [36–38]. After cultured overnight in DEME medium containing 10% (v: v) fetal bovine serum (FBS) with a 5% CO_2 incubator at 37 °C, HepG2 cells were treated with **DCT** (10 μM) for 30 min. Then washed with PBS ($pH = 7.4$) for at least three times, and Al^{3+} (40 μM) was added and incubated for another 30 min. As shown in Fig. 8, the cell viability showed a slight decrease and cell morphology kept consistency in the presence of **DCT**, considering that the cytotoxicity of **DCT** was negligible. The HepG2 cells incubated with **DCT** (10 μM) for 30 min at 37 °C showed nearly non-fluorescence. A obvious blue fluorescence was appeared in HepG2 cells after the addition of Al^{3+} (40 μM). The results were well accorded with the phenomenon in aqueous solution, revealed that **DCT** owns superior membrane permeability and biocompatibility and could be used for imaging Al^{3+} in living cells.

3.5. *Comparied with other probes*

The LOD of probe **DCT** is 82 nM. The result was comparable to or better than some of the reported methods. As showed in Table 1, for example, prof. Yang reported a probe based on naphthalene imide with the binding constant (K_a) was calculated to be $5.64 \times 10^4\ M^{-1}$ [19], which was one percent of our method. (4-(diethylamino)-2-hydroxybenzylidene)isoquinoline-1-carbohydrazide was designed by Xu's group with the detection limit of 80.8 nM, which was comparable with our probe (82 nM), but the reaction time was not discussed [21]. Prof. Varma designed a colorimetric probe for Al(III) ions, which the detection limit was 0.8 μM [34]. Compared with these, probe in my work has higher sensitivity and fast reaction time in aqueous. Besides, the binding constant of **DCT** is above the average than most of the reported methods. In a word, **DCT** possessed a lower LOD and speediness reaction time, and could be applied in practical application.

4. Conclusion

A new fluorescent **DCT** based on coumarin for Al^{3+}, has been designed and synthesized. **DCT** was easy to synthesize and the recognition process brought evident color changes from colorless to blue under 365 UV lamp. The detection limit was estimated as low as 82 nM and **DCT** showed a high affinity to Al^{3+} which the binding constant was of $5.04 \times 10^6\ M^{-1}$ according to a type of 1 : 1. The binding mechanism was further verified by DFT study. Moreover, **DCT** was applied as a effective fluorescence probe for bioimaging of Al^{3+} in vitro. This method was reported a new receptor toward Al^{3+}, and could be used in practical application.

Table 1
The comparison of **DCT** with other reported probes in the literature.

Association constant/M^{-1}	LOD/M	Stoichiometric ratio	Application	Reaction media	Reference
5.64×10^4	1.3×10^{-5}	1:1	Living cells imaging	Methanol	[19]
4.87×10^4	3.66×10^{-8}	1:1	Living cells imaging	Water	[20]
–	8.08×10^{-8}	2:1	Living cells imaging	Methanol	[21]
2.91×10^3	2.2×10^{-8}	1:1	–	DMSO:H_2O (1:9,*v*/*v*)	[30]
–	2.9×10^{-6}	1:1	Living cells imaging	DMSO:H_2O (1:1,*v*/*v*)	[31]
1.67×10^5	1.04×10^{-7} (480 nm) 4.17×10^{-6} (590 nm)	1:1	Living cells imaging	water-acetonitrile (4:1, v/v)	[32]
1×10^5	–	1:1	Living cells imaging	DMF:PBS (1:9,*v*/*v*) pH7.4	[33]
–	8×10^{-7}	1:1	tap water samples	Acetonitrile:water (95:5, v/v)	[34]
3.65×10^9	1.09×10^{-9}	1:1	Living cells imaging	Tris-HCl pH7.4	[36]
5.04×10^6	8.2×10^{-8}	1:1	Living cells imaging	CH_3CH_2OH - H_2O (6 : 4, v/v)	This work

Acknowledgements

This work is financially supported by the Six Talent Peak Project in Jiangsu Province (SWYY-063) and sponsored by Qing Lan Project of Jiangsu Province. Moreover, we also thank Turnitin (http://shidai.bi-ye.net/Turnitin/) for duplicate checking during the preparation of this manuscript.

Appendix A. Supplementary data

Supplementary data to this article can be found online at https://doi.org/10.1016/j.molstruc.2019.07.048.

References

[1] S. Das, M. Duttab, D. Das, Fluorescent probes for selective determination of trace level Al^{3+}: recent developments and future prospects, Anal. Methods. 5 (2013) 6262–6285.

[2] B. Valeur, I. Leray, Design principles of fluorescent molecular sensors for cation recognition, Coord. Chem. Rev. 205 (1) (2000) 3–40.

[3] Q. Zhu, L.L., L. Mu, X. Zeng, G. Wei, A ratiometric Al^{3+} ion probe based on the coumarin-quinoline FRET system, J. Photochem. Photobiol., A 328 (2016) 217–224.

[4] C. Meriño-Gergichevich, M. Alberdi, A.G. Ivanov, M. Reyes-Díaz, Al^{3+}-Ca^{2+} Interaction in piants growing in acid solids: al-phytotoxicity response to calcareous amendments, Plant Nutr. Soil Sci. 10 (2010), 217-213.

[5] M.L. Mora, M.A. Alfaro, S.C. Jarvis, R. Demanet, P. Cartes, Soil aluminium availability in Andisols of southern Chile and its effect on forage production and animal metabolism, Soil Use Manag. 22 (2006) 95–101.

[6] S. Dey, S. Halder, A. Mukherjee, K. Ghosh, P. Roy, Development of highly selective chemosensor for Al $^{3+}$: effect of substituent and biological application, Sens. Actuators B Chem. 215 (2015) 196–205.

[7] I. Narin, M. Tuzen, M. Soylak, Aluminium determination in environmental samples by graphite furnace atomic absorption spectrometry after solid phase extraction on Amberlite XAD-1180/pyrocatechol violet chelating resin, Talanta 63 (2004) 411–419.

[8] F. Zheng, B. Hu, Silica-coated magnetic nanoparticles modified withγ-mercaptopropyltrimethoxysilane for fast and selective solid phase extraction of trace amounts of Cd, Cu, Hg, and Pb in environmental and biological samples prior to their determination by inductively coupled plasma mass spectrometry, Spectrochim. Acta, Part B 63 (2008) 437–444.

[9] F. Thomas, A. Maslon, J.Y. Bottero, J. Rouiller, F. Montlgny, F. Genévrlere, Aluminum(III) speciation with hydroxy carboxylic acids. Aluminum-27 NMR study, Environ. Sci. Technol. 27 (1993) 2511–2516.

[10] D. Marino, J. Ingle, Determination of chlorine in water by luminol chemiluminescence, Anal. Chem. 53 (1981) 455–458.

[11] W.H. Ding, W. Cao, X.J. Zheng, D.C. Fang, W.T. Wong, L.P. Jin, A highly Selective fluorescent chemosensor for AlIII ion and fluorescent species formed in the solution, Inorg. Chem. 52 (2013) 7320–7322.

[12] V.K. Gupt, A.K. Singh, L.K. Kumawat, Thiazole Schiff base turn-on fluorescent chemosensor for Al^{3+} ion, Sens. Actuators B Chem. 195 (2014) 98–108.

[13] X. Sun, Y.W. Wang, Y. Peng, A selective and ratiometric bifunctional fluorescent probe for Al^{3+} ion and proton, Org. Lett. 14 (2012) 3420–3423.

[14] S. Chen, Y.M. Fang, Q. Xiao, J. Li, S.B. Li, H.J. Chen, J.J. Sun, H.H. Yang, Rapid visual detection of aluminium ion using citrate capped gold nanoparticles, Analyst 137 (2012) 2021–2023.

[15] L.N. Wang, W.W. Qin, X.L. Tang, W. Dou, W.S. Liu, Q.F. Teng, X.J. Yao, A selective, cell-permeable fluorescent probe for Al3+ in living cells, Org. Biomol. Chem. 8 (2010) 3751–3758.

[16] Y.W. Wang, M.X. Yu, Y.H. Yu, Z.P. Bai, Z. Shen, F.Y. Li, X.Z. You, A novel NIR violanthrone derivative with high electron-deficiency: effect of fluorescence on dicyanomethylene substitution, Tetrahedron Lett. 50 (2009) 6169–6172.

[17] X.G. Liu, Z.C. Xu, J.M. Cole, Molecular design of UV-vis absorption and emission properties in organic fluorophores: towards larger bathochromic shifts, enhanced molar extinction coefficients and greater Stokes shifts, cole, J. Phys. Chem. C 117 (2013) 16584–16595.

[18] O. Alici, S. Erdemir, A cyanobiphenyl containing fluorescence turn on sensor for Al^{3+} ion in CH$_3$CN-water, Sens. Actuators B Chem. 208 (2015) 159–163.

[19] X. l. Yue, C.R. Li, Z.Y. Yang, A novel Schiff-base fluorescent probe based on 1,8-naphthyridine and naphthalimide for Al^{3+}, Inorg. Chim. Acta 464 (2017) 167–171.

[20] F. Yu, L.J. Hou, L.Y. Qin, J.B. Chao, Y. Wang, W.J. Jin, A new colorimetric and turn-on fluorescent chemosensor for Al^{3+} in aqueous medium and its application in live-cell imaging, J. Photochem. Photobiol. A Chem. 315 (2016) 8–13.

[21] Y. Wang, Z.Y. Ma, D.L. Zhang, J.L. Deng, X. Chen, Highly selective and sensitive turn-on fluorescent sensor for detection of Al^{3+} based on quinoline-base Schiff base, Spectrochim. Acta A. 195 (2018) 157–164.

[22] A.B. Othman, J.W. Lee, Y.D. Huh, R. Abidi, J.S. Kim, J. Vicens, A novel pyrenyl-appended tricalix[4]arene for fluorescence-sensing of Al(III), Tetrahedron 63 (2017) 10793–10800.

[23] F.W. Hau, X. He, W.H. Lam, V.W. Yam, Highly selective ion probe for Al^{3+} based on Au(I)-Au(I) interactions in a bis-alkynylcalix[4]arene Au(I) isocyanide scaffold, Chem. Commun. 47 (2011) 8778–8780.

[24] S.H. Kim, H.S. Choi, J. Kim, S.J. Lee, D.T. Quang, J.S. Kim, Novel optical/electrochemical selective 1,2,3-triazole ring-appended chemosensor for the Al^{3+} ion, Org. Lett. 12 (2010) 560–563.

[25] W.L. Wang, Y.L. Yan, Q.M. Wang, A fluorescence turn - on probe for Al(III) based on naphthaldehy-derived, Chem. Lett. 46 (2017) 1605–1607.

[26] M. Ali, M. Jha, S.K. Das, S.K. Saha, Hydrogen-bond-induced microstructural transition of ionic micelles in the presence of neutral naphthols: pH dependent morphology and location of surface activity, J. Phys. Chem. B 113 (2009) 15563–15571.

[27] Q.M. Wang, W. Gao, X.H. Tang, Y. Liu, Y. Li, A fluorescence turn-on sensor for aluminum ion by a naphthaldehyde derivative, J. Mol. Struct. 1109 (2016) 127–130.

[28] X.L. Yue, Z.Q. Wang, C.R. Li, A highly selective and sensitive fluorescent chemosensor and its application for rapid on-site detection of Al^{3+}, Spectrochim. Acta A 193 (2018) 415–421.

[29] Q.M. Wang, W. Gao, Y. Li, T.T. Yang, Y. Ju, X.H. Tang, Highly sensitive and selective fluorescent "turn-on" probe for determination of aluminum ion in aqueous solution, Spectrosc. Lett. 49 (2) (2016) 80–84.

[30] A. Dhara, A. Jana, N. Guchhait, Susanta K. Kar, Isatin appended rhodamine scaffold as an efficient chemical tool to detect selectively Al^{3+}, J. Lumin. 154 (2014) 369–375.

[31] A. Thangaraj, K.S.K. Ashok, K.S. Suban, A new Al^{3+} selective fluorescent turn-on sensor based on hydrazide-naphthalic anhydride conjugate and its application in live cells imaging, Spectrochim. Acta A 204 (2018) 105–112.

[32] R. Singh, S. Samanta, P. Mullick, A. Ramesh, G. Das, Al^{3+} sensing through different turn-on emission signals vis-à-vis two different excitations: applications in biological and environmental realms, Anal. Chim. Acta 1025 (2018) 172–180.

[33] X.P. Ye, S.B. Sun, Y. Li, L.H. Zhi, W.N. Wu, Y. Wang, A highly sensitive, single selective, fluorescent sensor for Al^{3+} detection and its application in living cell imaging, J. Lumin. 155 (2014) 180–184.

[34] B. Jisha, M.R. Resmi, R.J. Maya, R. Luxmi Varma, Colorimetric detection of Al(III) ions based on triethylene glycol appended 8-propyloxy quinoline ester, Tetrahedron Lett. 54 (2013) 4232–4236.

[35] J.H. Ye, J. Liu, Z.H. Wang, Y. Bai, W.C. Zhang, W.J. He, A new Fe^{3+} fluorescent chemosensor based on aggregation-induced emission, Tetrahedron Lett. 55 (2014) 3688–3692.

[36] S.R. Gupta, P. Singh, B. Koch, V.P. Singh, A water soluble, highly sensitive and selective fluorescent probe for Al^{3+} ions and its application in live cell imaging, J. Photochem. Photobiol. A Chem. 348 (2017) 246–254.

[37] C. Nuñez, R. Bastida, A. Macais, E. Bertolo, L. Fernandes, J.L. Capelo, C. Lodeiro, Synthesis, characterization, and fluorescence behavior of four novel-macrocyclic emissive ligands containing a flexible 8-hydroxyquinoline unit, Tetrahedron 65 (2009) 6179–6188.

[38] D.P. Singh, R. Dwivedia, A.K. Singh, A dihydrazone based "turn-on" fluorescent probe for selective determination of Al^{3+} ions in aqueous ethanol, Sens. Actuators B Chem. 238 (2017) 128–137.

[39] D.S. Ranade, A.M. Bapat, S.N. Ramteke, B.N. Joshi, P. Roussel, A. Tomas, P. Deschamps, P.P. Kulkarni, Thiosemicarbazone modification of 3-acetyl coumarin inhibits Aβ peptide aggregation and protect against Aβ-induced cytotoxicity, Eur. J. Med. Chem. 121 (2016) 803–809.

[40] J. Chen, W. Liu, H. Xu, J. Wu, X. Tang, Z. Fan, P. Wang, Synthesis and properties of fluorescence dyes: tetracyclic pyrazolo[3,4-b]pyridine-based coumarin chromophores with intramolecular charge transfer character, J. Org. Chem. 77 (2012) 3475–3482.

[41] G. He, J. Li, Z. Wang, C. Liu, X. Liu, L. Ji, C. Xie, Q. Wang, Synthesis of a fluorogenic probe for thiols based on a coumarin schiff base copper complex and its use for the detection of glutathione, Tetrahedron 73 (2017) 272–277.

[42] E.S. Elzanfaly, A.S. Saad, A.B. Abd-Elaleem, Combining the isoabsorptive point in the ratio spectrum and the smart ratio difference methods for a single step determination of compounds with overlapped spectra, Spectrochim. Acta A Mol. Biomol. Spectrosc. 95 (2012) 188–192.

[43] Q.M. Wang, H.F. Sun, L. Jin, W.L. Wang, Z.H. Zhang, Y.L. Chen, A novel turn on and reversible sensor for Al^{3+} and its applications in bioimaging, J. Lumin. 203 (2018) 113–120.

[44] Y. Li, Q. Niu, T. Wei, T.D. Li, Novel thiophene-based colorimetric and fluorescent turn-on sensor for highly sensitive and selective simultaneous detection of Al^{3+} and Zn^{2+} in water and food samples and its application in bioimaging, Anal. Chim. Acta 1049 (2019) 196–212.

[45] M.A. Withersby, A.J. Blake, N.R. Champness, P.A. Cooke, P. Hubberstey, W.S. Li, M. Schroder, Solvent control in the synthesis of 3,6-bis(pyridine-3-yl)-1,2,4,5-tetrazine-bridged cadmium(II) and zinc(II) coordination polymers, Inorg. Chem. 38 (1999) 2259–2266.

[46] L.J. Daumann, K.E. Dalle, G. Schenk, R.P. McGeary, P.V. Bernhardt, D.L. Ollis, L.R. Gahan, The role of ZneOR and ZneOH nucleophiles and influence of parasubstituents in the reactions of binuclear phosphatase mimetics, Dalton Trans. 41 (2012) 1695–1708.

[47] F. Wang, J.H. Moon, R. Nandhakumar, B.T. Kang, D. Kim, K.M. Kim, J.Y. Lee, J. Yoon, Zn^{2+}-induced conformational changes in a binaphthyl-pyrene derivative monitored by using fluorescence and CD spectroscopy, Chem. Commun. 49 (2013) 7228–7230.

[48] Q. Zhang, Q. Jiao, Q. Zhang, A novel crown ether-acylhydrazone turn-on

fluorescent chemosensor for Al^{3+} ion, Spectrochim. Acta A Mol. Biomol. Spectrosc. 211 (2019) 1–8.

[49] Z.H. Xu, Y. Wang, Y. Wang, AIE active salicylaldehyde-based hydrazone: a novel single-molecule multianalyte (Al^{3+} or Cu^{2+}) sensor in different solvents, Spectrochim. Acta A Mol. Biomol. Spectrosc. 212 (2019) 146–154.

[50] S.K. Sheet, B. Sen, R. Thounaojam, Highly selective light-up Al^{3+} sensing by a coumarin based Schiff base probe: subsequent phosphate sensing DNA binding and live cell imaging, J. Photochem. Photobiol. A Chem. 332 (2017) 101–111.